Am J Clin Exp Immunol 2025;14(1):1-13
www.ajcei.us /ISSN:2164-7712/AJCEI0159715

Original Article

Identification of immune infiltration-related ZNF480 for predicting prognosis in breast cancer

Tong Zhou[1,2*], Yanqiu Zhang[3*], Jun Cao[1], Qingqin Tang[1], Yuting Liang[1], Sheng Zhang[1], Mengyuan Hu[1,2], Bin Feng[1], Jieyu Jin[1]

[1]Center for Clinical Laboratory, The First Affiliated Hospital of Soochow University, Suzhou, Jiangsu, The People's Republic of China; [2]Medical College of Soochow University, Suzhou, Jiangsu, The People's Republic of China; [3]Institute of Clinical Pharmacology, Anhui Medical University, Key Laboratory of Anti-inflammatory and Immune Medicine, Ministry of Education, Anhui Collaborative Innovation Center of Anti-inflammatory and Immune Medicine, Hefei, Anhui, The People's Republic of China. [*]Equal contributors.

Received August 9, 2024; Accepted January 22, 2025; Epub February 25, 2025; Published February 28, 2025

Abstract: Background: Breast cancer is one of the most common cancers in women with high morbidity and mortality. ZNF480, a member of the KRAB-ZNFs family, correlates with cancer progression. However, its role in the development and progression of breast cancer remains unclear. Methods: We utilized transcriptomic and clinical data from The Cancer Genome Atlas (TCGA) and Genotype Tissue Expression (GTEx) databases of breast cancer patients to investigate the potential pro-cancer role of ZNF480, including differential expression of ZNF480 in breast cancer, prognostic value, clinicopathological features, immune cell infiltration relevance and function enrichment analysis. Results: Our results indicate that ZNF480 is upregulated in breast cancer and is correlations with survival, clinical stage, race and tumor subtype in breast cancer patients. Additionally, immune infiltration analysis revealed significant negative correlations between ZNF480 expression and multiple tumor infiltrating immune cells, including aDC, B cells, CD8 T cells, Cytotoxic cells, DC, iDC, Macrophages, Neutrophils, NK CD56bright cells, NK CD56dim cells, NK cells, pDC, T cells, Tem, TFH and Th1 cells, whereas a significant positive correlation was observed with the infiltration of T helper cells, Tcm, Tgd and Th2 cells. Furthermore, functional enrichment analysis indicated that ZNF480 may be involved in Angiogenesis, Allograft rejection, TNFα signaling via NFκB, Coagulation, IL6 Jak STAT3 signaling, Inflammatory response, Interferon gamma response and other processes. Conclusion: ZNF480 is highly expressed in breast cancer and correlates with immune cell infiltration, and may be a candidate prognostic biomarker, which may assist in breast cancer treatment.

Keywords: ZNF480, breast cancer, prognosis, immune infiltration, bioinformatics

Introduction

According to global cancer statistics, there were almost 2.3 million new cases of breast cancer in women in 2022, accounting for 11.6% of all cancer cases and second only to lung cancer. It ranks first in the incidence and mortality of female tumors [1]. Despite remarkable improvements in the diagnosis and treatment of breast cancer, the increasing complexity of the disease poses a challenge to all resource settings [2]. At the molecular level, breast cancer exhibits heterogeneity and diverse gene expression patterns, which presumably contribute to differences in tumor behavior and prognosis [3]. Therefore, exploring novel molecular targets and the role of immune-related genes would help guide drug usage or treatment strategies.

Zinc finger proteins (ZNFs), the largest family of transcription factors and epigenetic regulators in mammals, play critical roles in embryonic development, epigenetic modifications, immune system regulation, and cancer progression [4]. Within this family, Kruppel-associated box zinc finger proteins (KRAB-ZNFs) represent the largest subfamily, characterized by their ability to bind specific DNA sequences through zinc finger motifs and recruit inhibitory complexes via the KRAB domain, thereby promoting tumor cell proliferation, invasion, and immune evasion

https://doi.org/10.62347/LNKO2367

Table 1. The abbreviations and corresponding full names of 33 cancers

Abbreviation	Cancer Type
ACC	Adrenocortical carcinoma
BLCA	Bladder urothelial carcinoma
BRCA	Breast invasive carcinoma
CESC	Cervical squamous cell carcinoma and endocervical Adenocarcinoma
CHOL	Cholangiocarcinoma
COAD	Colon adenocarcinoma
DLBC	Lymphoid neoplasm diffuse Large B-cell lymphoma
ESCA	Esophageal carcinoma
GBM	Glioblastoma multiforme
HNSC	Head and neck squamous cell carcinoma
KICH	Kidney chromophobe
KIRC	Kidney renal clear cell carcinoma
KIRP	Kidney renal papillary cell carcinoma
LAML	Acute myeloid leukemia
LGG	Brain lower grade glioma
LIHC	Liver hepatocellular carcinoma
LUAD	Lung adenocarcinoma
LUSC	Lung squamous cell carcinoma
MESO	Mesothelioma
OV	Ovarian serous cystadenocarcinoma
PAAD	Pancreatic adenocarcinoma
PCPG	Pheochromocytoma and paraganglioma
PRAD	Prostate adenocarcinoma
READ	Rectum adenocarcinoma
SARC	Sarcoma
SKCM	Skin cutaneous melanoma
STAD	Stomach adenocarcinoma
TGCT	Testicular germ cell tumors
THCA	Thyroid carcinoma
THYM	Thymoma
UCEC	Uterine corpus endometrial carcinoma
UCS	Uterine carcinosarcoma
UVM	Uveal melanoma

[5, 6]. Despite the established involvement of ZNFs in breast cancer progression, the complexity of the KRAB-ZNF gene superfamily, particularly the role of ZNF480 - expressed in cardiac, skeletal muscle, pancreatic, and placental tissues remains underexplored, necessitating further research to understand its mutations and their impact on patient prognosis [4, 7, 8].

In this study, we aimed to elucidate the role of immune cell infiltration in breast cancer via bioinformatics by analyzing TCGA and GTEx patient data, focusing on transcriptome and clinical information. Our innovative approach integrates large-scale gene expression with clinical outcomes to identify and validate immune cell subtypes related to breast cancer progression, precisely understand their influence on the tumor microenvironment, and explore ZNF480's potential function. This study has deepened the understanding of the immune microenvironment and provided a scientific basis for new treatment methods.

Materials and methods

Dataset analyses

The RNA-sequencing (Seq) data and clinical records were obtained from the Cancer Genome Atlas (TCGA) database and the Genotype Tissue Expression Project (GTEx) database. Subsequently, the database was utilized to investigate ZNF480 expression in breast cancer and for pan-cancer analysis. The abbreviations of 33 types of tumors are shown in **Table 1**.

Survival analysis

In this study, Kaplan-Meier survival curves combined with the Cox regression analysis were utilized to assess the survival outcomes of patients using R package survminer and survival. The association between ZNF480 expression and patient prognosis, including overall survival (OS), disease-specific survival (DSS) and progress-free interval (PFI), as well as the association between ZNF480 expression and the prognosis of patients with different subtypes of breast cancer were investigated. Furthermore, we employed the ggplot2 package in R software version 4.2.1 to generate forest plots to visualize the pan-cancer prognostic analysis.

Differential gene expression analysis

The breast cancer patients in the TCGA dataset were stratified into high and low ZNF480 expression groups based on the optimal cut-off value. The DESeq2 package in R language was utilized to analyze the differential gene expressions between these two groups, aiming to identify differentially expressed genes (DEGs) [9-11]. The screening criteria for DEGs included an adjusted p value <0.05 and |log2-fold-change (FC)|>1.

Functional enrichment analysis

The DEGs were subjected to Gene Ontology (GO) and Kyoto Encyclopedia of Genes and Genomes (KEGG) enrichment analysis, aiming to elucidate their distribution across biological processes, molecular functions, and cellular components [12, 13]. Additionally, Gene Set Enrichment Analysis (GSEA) of Hallmark gene sets and C2 curated gene sets were employed to investigate signaling pathway enrichment to comprehensively assess the expression patterns of all genes [14]. This comprehensive analysis provides valuable insights into the functional properties of the ZNF480. A significance criterion of an adjusted p value <0.05 was applied in these analyses.

Immune cell infiltration analysis

Using the ssGSEA method in the R package GSVA version 1.46.0 [15], this study employed a panel of 24 immune cell markers to evaluate the extent of immune cell infiltration based on data provided by Bindea et al.'s [16] article published in Immunity journal. We conducted a Wilcoxon rank sum test to compare the disparity in immune infiltration levels between the high expression group of ZNF480 and the low expression group of ZNF480. In addition, the estimate package was employed to calculate the stromal scores, immune scores and estimate scores for the samples [17].

Statistical analysis

The data analyses were performed using R software, version 4.2.1. For comparing differences between groups, the choice of statistical test (Wilcoxon rank-sum test or paired sample t-test) was based on the distribution properties of the data. To assess correlations between variables, either Pearson correlation test or Spearman rank correlation test was employed depending on the data distribution. Survival analyses were performed using Kaplan-Meyer survival curves and Cox regression. P value <0.05 was considered statistically significant in all analyses.

Results

Higher ZNF480 expression levels in cancerous than in noncancerous tissues

The findings of pan-cancer analysis in the TCGA database revealed a general upregulation in the expression levels of the ZNF480 gene across a diverse range of tumor types, including BLCA, BRCA, CHOL, COAD, ESCA, GBM, HNSC, LIHC, LUAD, LUSC, PRAD, READ, STAD and UCEC, compared to paraneoplastic tissues (**Figure 1A**). Due to the lack of normal tissue in the TCGA database, we merged the TCGA and GTEx databases, and the results further revealed conspicuous upregulation of ZNF480 across diverse tumor types, encompassing ACC, BLCA, BRCA, CESC, CHOL, COAD, DLBC, ESCA, GBM, HNSC, KICH, KIRP, LGG, LIHC, LUAD, LUSC, OV, PAAD, PRAD, READ, SKCM, STAD, TGCT, THYM, UCEC and UCS (**Figure 1B**).

In addition, the expression levels of ZNF480 were markedly elevated in breast cancer compared to normal breast tissues (**Figure 1C**). The expression levels of the ZNF480 gene exhibited a consistent up-regulation in paired breast tissue samples (**Figure 1D**). The receiver operating characteristic (ROC) curve analysis confirmed the significant diagnostic potential of ZNF480 gene expression in breast cancer, effectively distinguishing tumor tissues from normal tissues. The analysis results demonstrated an area under the curve (AUC) of 0.868 for ZNF480, with a 95% confidence interval (CI) ranging from 0.847 to 0.888, indicating its high accuracy and reliability (**Figure 1E**).

Value of ZNF480 overexpression in diagnosis and predicting prognosis

The forest plots generated from the Cox regression analysis revealed a significant association between OS and various cancer types. In the case of breast cancer, an increase in gene expression levels was found to be correlated with a deteriorating prognosis [P=0.0386, haz-

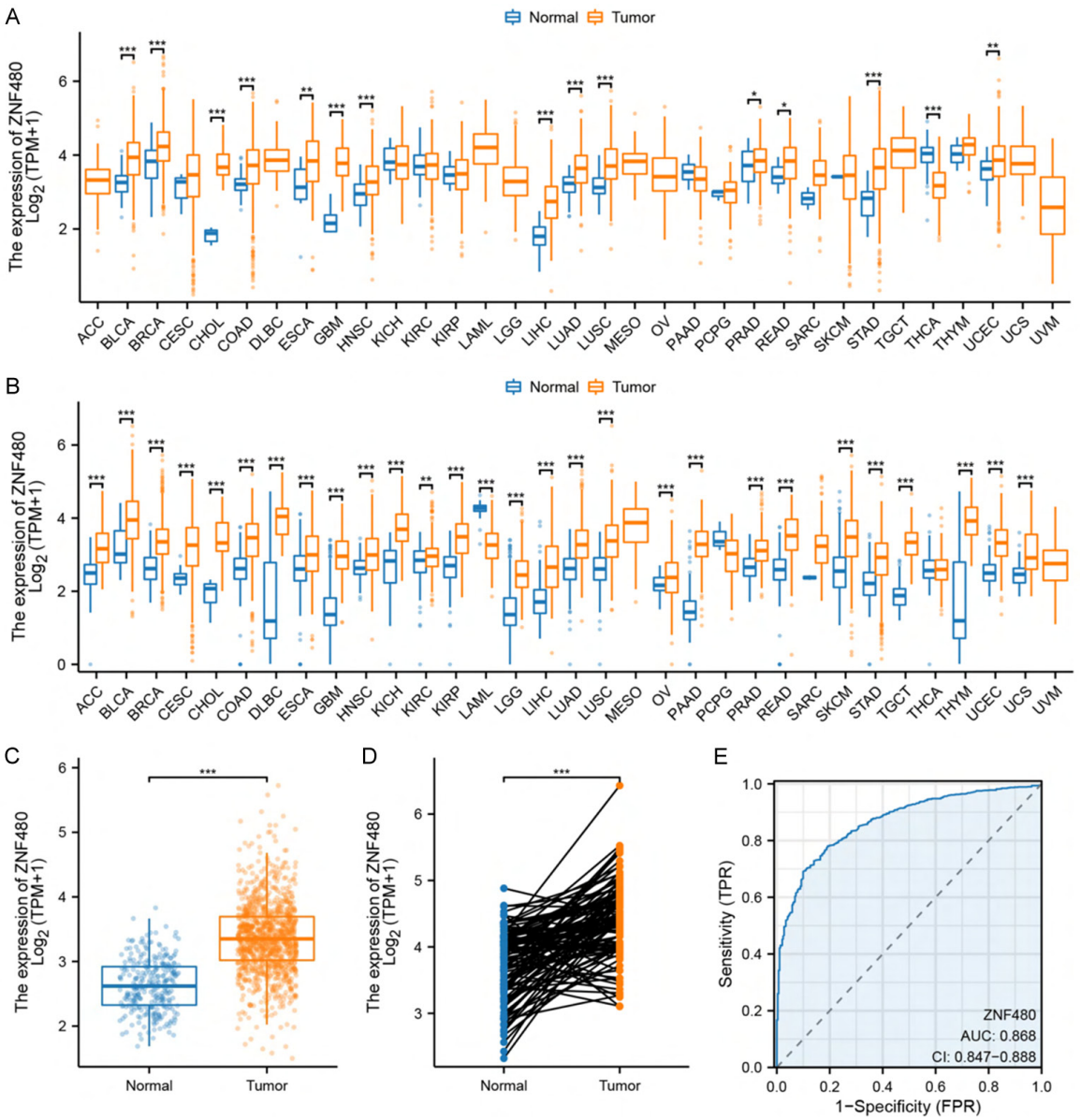

Figure 1. Expression levels of ZNF480 in different types of tumors and breast cancer. (A) ZNF480 expression levels in 33 types of cancer tissues and paraneoplastic tissues in TCGA databases. (B) ZNF480 expression levels in 33 types of cancer tissues and normal tissues in TCGA and GTEx databases. Expression of ZNF480 (C) in breast cancer and non-matched normal tissues in the TCGA and GTEx databases, and (D) in breast cancer and matched normal tissues in TCGA database. (E) The ROC curve of diagnosis to distinguish tumor from normal tissues. *P<0.05, **P<0.01, and ***P<0.001. ACC, Adrenocortical Carcinoma; BLCA, Bladder Urothelial Carcinoma; BRCA, Breast Invasive Carcinoma; CESC, Cervical Squamous Cell Carcinoma and Endocervical Adenocarcinoma; CHOL, Cholangiocarcinoma; COAD, Colon Adenocarcinoma; DLBC, Diffuse Large B-Cell Lymphoma; ESCA, Esophageal Carcinoma; GBM, Glioblastoma Multiforme; HNSC, Head and Neck Squamous Cell Carcinoma; KICH, Kidney Chromophobe; KIRP, Kidney Renal Clear Cell Carcinoma; LGG, Brain Lower Grade Glioma; LIHC, Liver Hepatocellular Carcinoma; LUAD, Lung Adenocarcinoma; LUSC, Lung Squamous Cell Carcinoma; OV, Ovarian Serous Cystadenocarcinoma; PAAD, Pancreatic Adenocarcinoma; PRAD, Prostate Adenocarcinoma; READ, Rectum Adenocarcinoma; SKCM, Skin Cutaneous Melanoma; STAD, Stomach Adenocarcinoma; TGCT, Testicular Germ Cell Tumors; THYM, Thymoma; UCEC, Uterine Corpus Endometrial Carcinoma; UCS, Uterine; UVM, Uveal Melanoma.

ard ratio (HR) =1.319, 95% CI=1.015-1.714] (**Figure 2A**).

The patients were categorized into high- and low-ZNF480 expression groups based on the

A

ZNF480 – Overall Survival

Group	Total(N)	HR(95% CI)	P value
ACC	79	1.229 (0.690 – 2.187)	0.4837
BLCA	411	0.831 (0.680 – 1.016)	0.0716
BRCA	1086	1.319 (1.015 – 1.714)	0.0386
CESC	306	1.137 (0.887 – 1.459)	0.3106
CHOL	35	0.418 (0.123 – 1.418)	0.1617
COAD	477	0.963 (0.785 – 1.181)	0.7146
DLBC	48	0.672 (0.177 – 2.558)	0.5605
ESCA	163	1.160 (0.837 – 1.608)	0.3741
GBM	168	0.794 (0.572 – 1.104)	0.1705
HNSC	503	1.000 (0.803 – 1.246)	0.9978
KICH	64	4.859 (1.437 – 16.425)	0.0110
KIRC	541	0.576 (0.446 – 0.744)	2.44e−05
KIRP	290	1.225 (0.745 – 2.013)	0.4242
LAML	139	0.879 (0.641 – 1.206)	0.4248
LGG	530	2.129 (1.611 – 2.814)	1.1e−07
LIHC	373	1.448 (1.110 – 1.889)	0.0063
LUAD	530	1.033 (0.788 – 1.354)	0.8126
LUSC	496	0.963 (0.767 – 1.208)	0.7446
MESO	86	1.540 (0.915 – 2.591)	0.1038
OV	379	0.963 (0.781 – 1.187)	0.7232
PAAD	179	1.653 (1.118 – 2.444)	0.0118
PCPG	184	0.426 (0.102 – 1.779)	0.2422
PRAD	501	2.101 (0.583 – 7.565)	0.2562
READ	166	0.780 (0.445 – 1.367)	0.3856
SARC	263	1.195 (0.844 – 1.692)	0.3160
SKCM	457	1.075 (0.923 – 1.252)	0.3523
STAD	370	1.050 (0.872 – 1.265)	0.6054
TGCT	139	0.257 (0.040 – 1.635)	0.1500
THCA	512	1.735 (0.630 – 4.776)	0.2862
THYM	119	0.196 (0.035 – 1.085)	0.0620
UCEC	553	1.166 (0.857 – 1.588)	0.3285
UCS	57	1.512 (0.881 – 2.597)	0.1339
UVM	80	1.512 (0.923 – 2.477)	0.1004

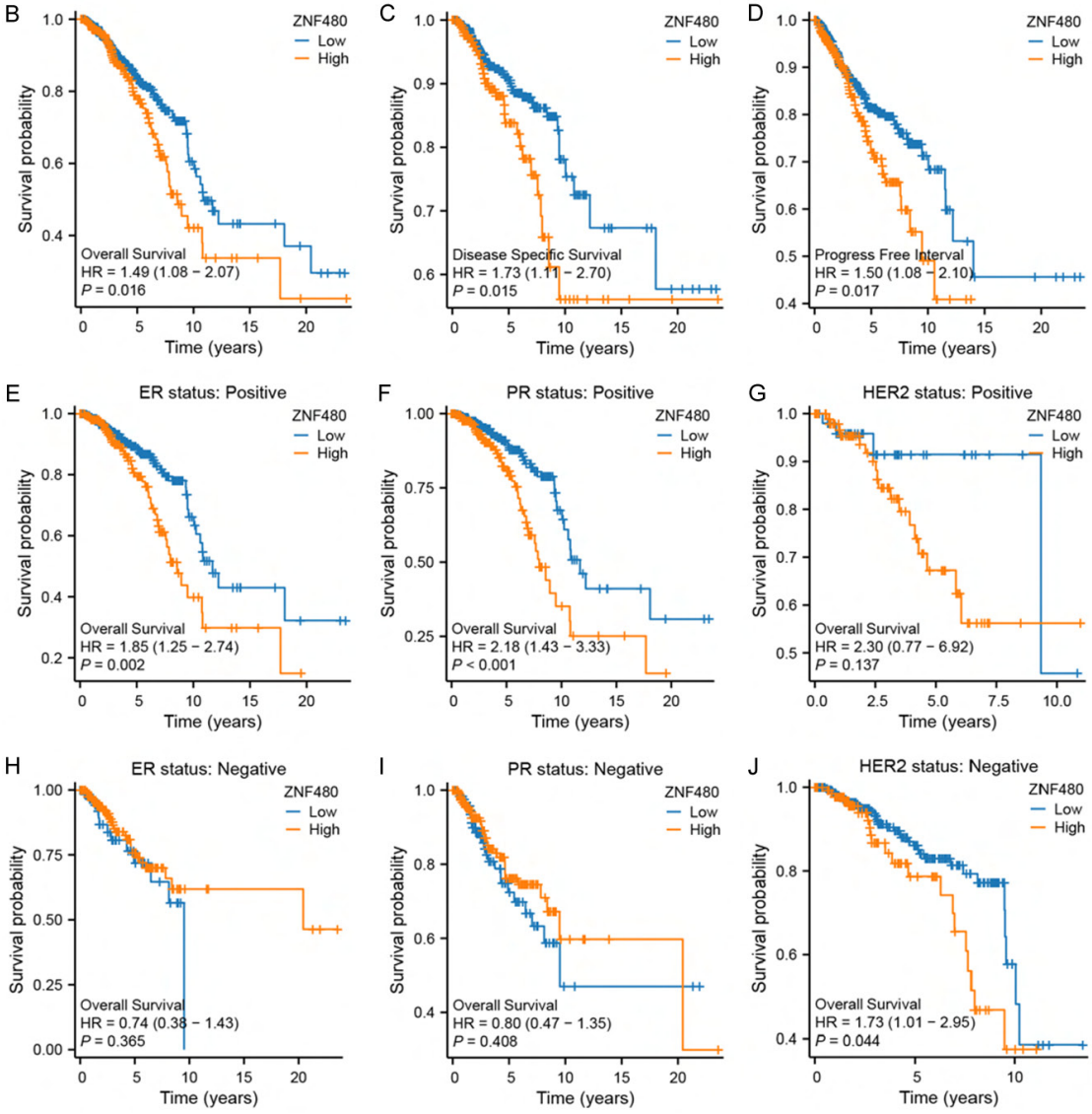

Figure 2. ZNF480 expression correlated with prognosis. (A) The forest map based on Cox regression analysis for OS. The (B) OS, (C) DSS, and (D) PFI survival curves comparing patients with high (orange) and low (blue) ZNF480 expression in breast cancer were plotted. ZNF480 expression level was associated with the OS of patients with (E) ER positive, (F) PR positive, (G) HER2 positive, (H) ER negative, (I) PR negative, and (J) HER2 negative.

optimal cut-off value. The association between the level of ZNF480 gene expression and the prognosis of breast cancer patients was assessed using the Kaplan-Meier survival curve method. The findings revealed a significant correlation between high ZNF480 expression and poor prognosis in breast cancer patients, particularly with regards to shorter OS (HR=1.49, 95% CI=1.08-2.07, P=0.016), lower DSS (HR=1.73, 95% CI=1.11-2.70, P=0.015), and PFI (HR=1.50, 95% CI=1.08-2.10, P=0017). These results emphasize the detrimental impact of ZNF480 gene expression on the prognosis of breast cancer patients and suggest its potential as an important guiding factor in clinical treatment (**Figure 2B-D**).

In addition, we further investigated the relationship between estrogen receptor (ER), progesterone receptor (PR), human epidermal growth factor receptor 2 (HER2) expression and ZNF480 expression in breast cancer patients. In ER-positive breast cancer patients, high ZNF480 expression was significantly associated with poor OS (HR=1.85, 95% CI=1.25-2.74, P=0.002) (**Figure 2E**). The same results were observed for PR-positive (HR=2.18, 95% CI=1.43-3.33, P<0.001), and HER2-negative (HR=1.73, 95% CI=1.01-2.95, P=0.044) and HER2-positive (HR=2.30, 95% CI=0.77-6.92, P=0.137) breast cancer cases. Remarkably, in HER2-positive breast cancer patients, there was no statistically significant difference in OS between those with high versus low ZNF480 expression (HR=2.30, 95% CI=0.77-6.92, P=0.137). Similar findings were observed in patients with ER-negative (HR=0.74, 95% CI=0.38-1.43, P=0.365) and PR-negative (HR=0.80, 95% CI=0.47-1.35, P=0.408) (**Figure 2E-J**).

Associations between ZNF480 expression and clinicopathologic variables

As illustrated in **Figure 3**, the expression of ZNF480 was found to be significantly associated with the T stage (normal vs. T1, P<0.001; normal vs. T2, P<0.001; normal vs. T3&T4, P<0.001; T1 vs. T3&T4, P<0.05; T2 vs. T3&T4, P<0.01), N stage (normal vs. N0, P<0.001; normal vs. N1, P<0.001; normal vs. N2, P<0.001; normal vs. N3, P<0.01), M stage (normal vs. M0, P<0.001; normal vs. M1, P<0.05; M0 vs. M1, non-significant), pathologic stage (normal vs. stage I, P<0.001; normal vs. stage II, P<0.001; normal vs. stage III&stage IV, P<0.001), race (normal vs. Asian, P<0.001; normal vs. White, P<0.001; Asian vs. Black or African American, P<0.001; White vs. Black or African American, P<0.001), PAM50 (normal vs. Basal, P<0.001; normal vs. Luminal A, P<0.001; normal vs. Luminal B, P<0.001; normal vs. HER2, P<0.001; Basal vs. Luminal A, P<0.01; Basal vs. Luminal B, P<0.001; Basal vs. HER2, P<0.001; Luminal A vs. Luminal B, P<0.001; Luminal A vs. HER2, P<0.05), ER status (normal vs. Negative, P<0.001; normal vs. Positive, P<0.001; Negative vs. Positive, P<0.05), PR status (normal vs. Negative, P<0.001; normal vs. Positive, P<0.001; Negative vs. Positive, P<0.01) and HER2 status (normal vs. Negative, P<0.001; normal vs. Positive, P<0.001).

Relationship between the expression of ZNF480 with immune infiltration level

The ssGSEA was employed to investigate the expression levels of the ZNF480 gene and its association with immune cell infiltration levels in breast cancer. Our analysis revealed that patients with high ZNF480 expression exhibited significantly lower levels of immune cell infiltration compared to those with low expression levels. The relative infiltration levels of activated dendritic cells (aDC), B cells, CD8 T cells, cytotoxic cells, dendritic cells (DC), immature dendritic cells (iDC), macrophages, neutrophils, natural killer (NK) CD56bright cells, NK CD56dim cells, NK cells, plasmacytoid dendritic cells (pDC), T cells, effector memory T cells (Tem), follicular helper T cells (TFH), and Th1 cells were significantly lower in the ZNF480 high-expression group, whereas the infiltration levels of T helper cells, central memory T cells (Tcm), gammadelta T cells (Tgd) and Th2 cells were significantly higher in the ZNF480 high-expression group (**Figure 4A**).

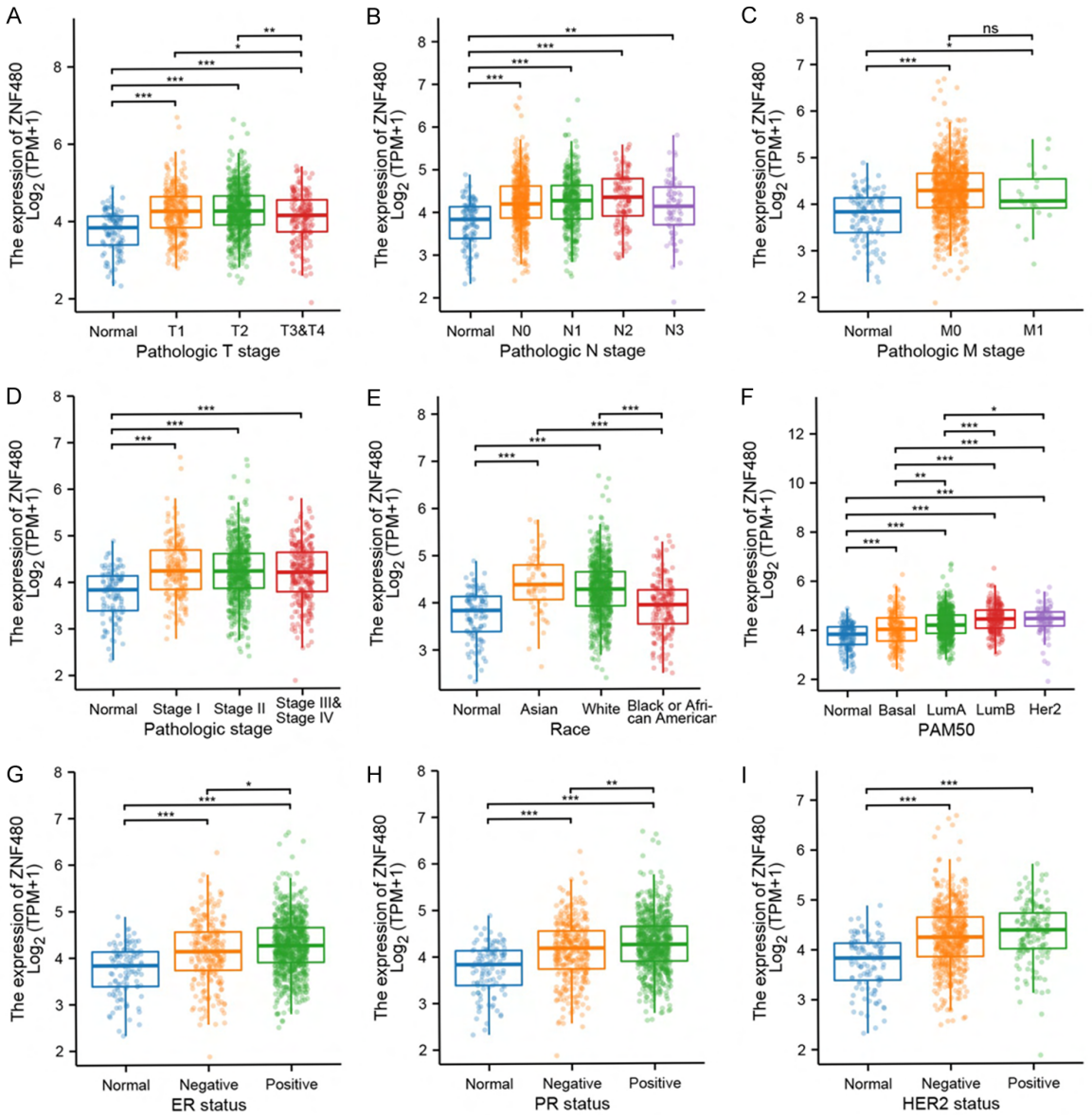

Figure 3. Relationship between the expression of ZNF480 and clinicopathologic variables. The expression of ZNF480 notably correlated with (A) T stage, (B) N stage, (C) M stage, (D) pathologic stage, (E) race, (F) PAM50, (G) ER status, (H) PR status and (I) HER2 status. *P<0.05, **P<0.01, and ***P<0.001.

The expression of ZNF480 exhibited a significant negative correlation with the level of immune cell infiltration by pDCs (r=-0.414, P<0.001). Conversely, there was a positive correlation between the expression of ZNF480 and the level of immune infiltration of T helper cells (r=0.319, P<0.001), as well as Tcm cells (r=0.371, P<0.001). However, weak correlations were observed with the infiltration levels of other cell types such as cytotoxic cells, DC, and CD8 T cells (**Figure 4B**).

Additionally, based on the results of Spearman correlation analysis, we observed a weak negative association between the expression level of ZNF480 and stromal score, which was statistically significant (r=-0.066, P=0.030). Furthermore, there was a weak to moderate negative correlation between the expression level of ZNF480 and both immune score (r=-0.233, P<0.001) and estimate score (r=-0.181, P<0.001) as indicated by the Spearman correlation coefficient (**Figure 4C-E**).

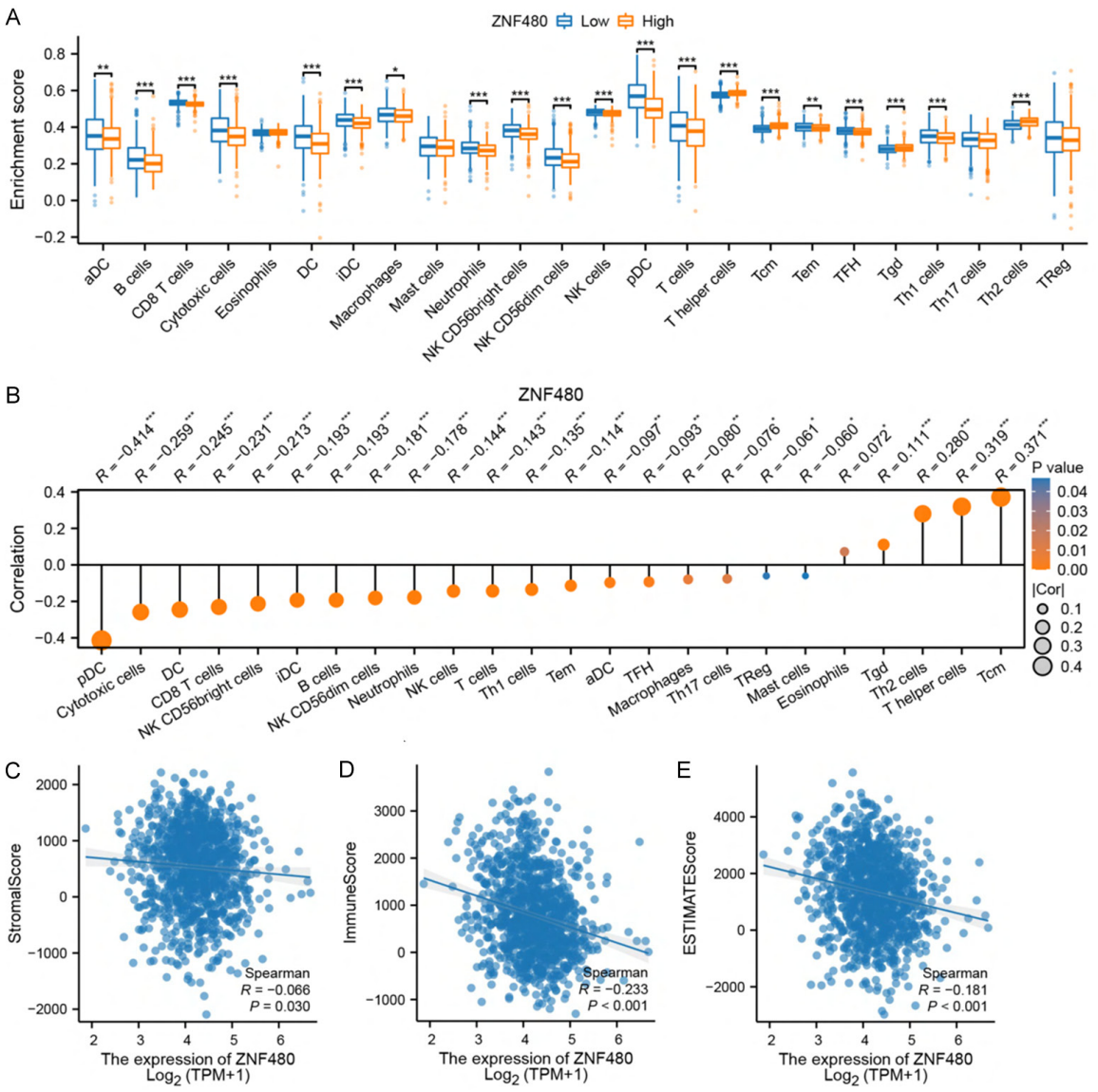

Figure 4. Association between ZNF480 expression and immune cell infiltration. (A) Association between ZNF480 expression with immune infiltration level. (B) Correlation between ZNF480 expression and relative abundance of 24 types of immune cell. The size of dot corresponds to the absolute Spearman's correlation coefficient values. Scatter plots based on the Spearman rank correlation coefficient between ZNF480 expression level and (C) stromal score, (D) immune score, and (E) estimate score. *P<0.05, **P<0.01, and ***P<0.001.

Identification of ZNF480-related genes and functional enrichment analysis

The volcano plot revealed that a total of 76 significantly upregulated genes (indicated in orange) and 449 significantly downregulated genes (indicated in blue) were obtained between the ZNF480 high- and low-expression groups (adjusted *p*-value <0.05, |Log2-FC|>1) (**Figure 5A**). The heatmap displayed the relationship between the top ten DEGs (CSN2, LALBA, SMR3B, APOA2, LCE1A, CPLX2, LACRT, KRT20, PAGE1 and CLVS2) and ZNF480 (**Figure 5B**).

Enrichment analysis of GO included three essential functional categories, namely biological processes, cellular components, and molecular functions. In terms of biological processes, significant terms comprised "keratinization", "antimicrobial humoral response", "humoral immune response", "keratinocyte differentiation", and "epidermal development". The cellular components category highlighted "blood

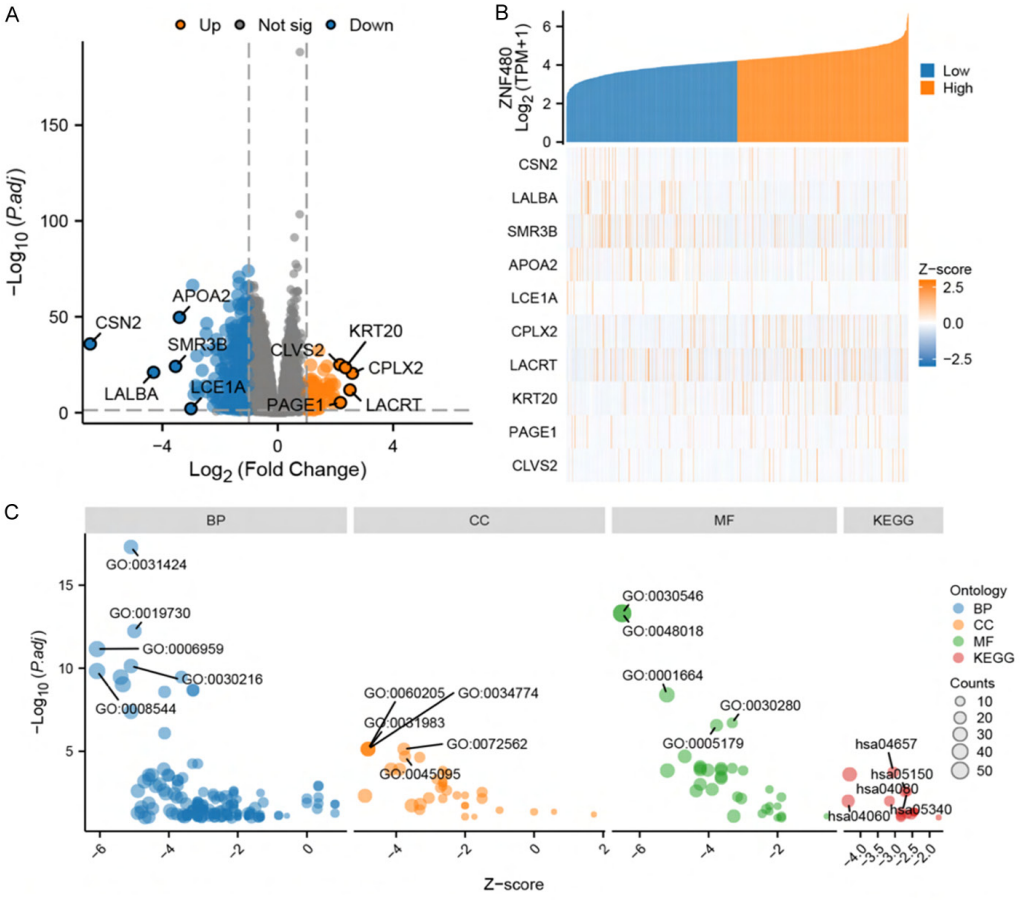

ID	Description
GO:0031424	keratinization
GO:0019730	antimicrobial humoral response
GO:0006959	humoral immune response
GO:0030216	keratinocyte differentiation
GO:0008544	epidermis development
GO:0072562	blood microparticle
GO:0034774	secretory granule lumen
GO:0060205	cytoplasmic vesicle lumen
GO:0031983	vesicle lumen
GO:0045095	keratin filament
GO:0048018	receptor ligand activity
GO:0030546	signaling receptor activator activity
GO:0001664	G protein-coupled receptor binding
GO:0030280	structural constituent of skin epidermis
GO:0005179	hormone activity
hsa04657	IL-17 signaling pathway
hsa04080	Neuroactive ligand-receptor interaction
hsa05150	Staphylococcus aureus infection
hsa05340	Primary immunodeficiency
hsa04060	Cytokine-cytokine receptor interaction

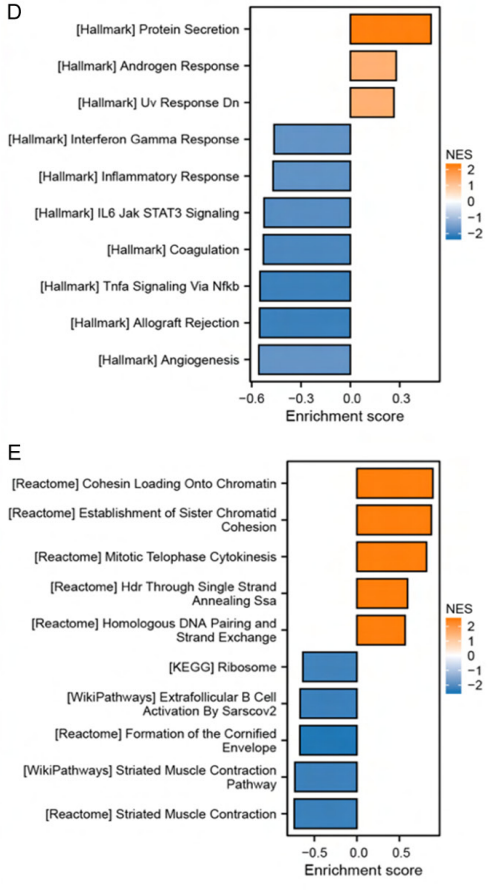

Figure 5. Functional annotations and predicted signaling pathways. A. Volcano plot of DEGs. Blue and red dots indicate the significantly down-regulated and up-regulated DEGs, respectively. B. Heatmap of correlation between ZNF480 expression and the top 10 DEGs. C. GO term and KEGG pathway enrichment analyses. D. GSEA analysis of Halmark gene sets. E. GSEA analysis of C2 curated gene sets. GO, Gene Ontology; KEGG, Kyoto Encyclopedia of Genes and Genomes; DEGs, differentially expressed genes.

Table 2. Functional annotation

ID	Description
GO:0031424	Keratinization
GO:0019730	Antimicrobial humoral response
GO:0006959	Humoral immune response
GO:0030216	Keratinocyte differentiation
GO:0008544	Epidermis development
GO:0072562	Blood microparticle
GO:0034774	Secretory granule lumen
GO:0060205	Cytoplasmic vesicle lumen
GO:0031983	Vesicle lumen
GO:0045095	Keratin filament
GO:0048018	Receptor ligand activity
GO:0030546	Signaling receptor activator activity
GO:0001664	G protein-coupled receptor binding
GO:0030280	Structural constituent of skin epidermis
GO:0005179	Hormone activity
hsa04657	IL-17 signaling pathway
hsa04080	Neuroactive ligand-receptor interaction
hsa05150	Staphylococcus aureus infection
hsa05340	Primary immunodeficiency
hsa04060	Cytokine-cytokine receptor interaction

microparticle", "secretory granule lumen", "cytoplasmic vesicle lumen", "vesicle lumen" and "keratin filament". Regarding molecular function roles that stood out were related to "receptor ligand activity", "signaling receptor activator activity", "G protein-coupled receptor binding", "structural components of skin epidermis" and "hormonal activity". Additionally, KEGG pathway analysis revealed that DEGs were significantly enriched in pathways such as "IL-17 signaling pathway", "neuroactive ligand-receptor interaction", "staphylococcus aureus infection", "primary immunodeficiency" and "cytokine-cytokine receptor interaction" (**Figure 5C** and **Table 2**).

To further reveal the potential pathways and biological processes by which ZNF480 may regulate breast cancer development and progression, GSEA analyses were performed on DEGs. As can be seen from **Figure 5D**, **5E**, pathways involved in angiogenesis, allograft rejection, TNFα signaling via NFκB, coagulation, IL6 Jak STAT3 signaling, inflammatory response, interferon gamma response, striated muscle contraction, striated muscle contraction pathway, formation of the cornified envelope, extrafollicular B cell activation by sarscov2 and ribosome pathway were inhibited in the ZNF480 high-expression group, whereas the pathways involved in protein secretion, androgen response, UV response DN, cohesin loading onto chromatin, establishment of sister chromated cohesion, mitotic telophase cytokinesis, HDR through single strand annealing SSA and homologous DNA pairing and strand exchange were activated (**Figure 5D**, **5E**).

Discussion

Breast cancer, a multifactorial disease driven by genetic and environmental determinants, presents significant heterogeneity. Despite advancements, the pathogenesis remains inadequately understood. Rising healthcare costs and new targeted therapies highlight the role of biomarkers in disease monitoring during and post-treatment [18]. Early biomarker identification and effective therapeutic strategies are critical for improving patient survival. ZNF480, a key transcription factor in embryogenesis, regulates cell fate and tissue morphogenesis [19]. However, its role in cancer, particularly in initiation, progression, and immune infiltration, remains to be elucidated. This study aims to elucidate ZNF480's functions, potentially informing breast cancer diagnosis and treatment.

In this study, we performed a comprehensive analysis of TCGA and GTEx datasets to evaluate ZNF480 expression in breast cancer versus adjacent normal tissues. Our results demonstrate a significant upregulation of ZNF480 in breast cancer, underscoring its potential as a biomarker. Elevated ZNF480 expression correlates with poor clinical outcomes, including OS, DSS, and PFI, with its prognostic impact varying across breast cancer subtypes. This finding is consistent with the high expression levels of ZNF480 observed in low-grade gliomas (LGG)

and the associated poor prognosis for patients [4].

The development and progression of breast cancer is propelled by an intricate network encompassing receptor tyrosine kinases (RTKs) as well as steroid hormone receptors, notably estrogen receptors (ER) and progesterone receptors (PR). The interplay among these receptors may significantly impact. Our study observed that high ZNF480 levels are associated with lower OS in ER- and PR-positive patients, indicating poor prognosis, while improved survival is observed in ER- and PR-negative patients. However, elevated ZNF480 expression predicts poor OS in both HER2-positive and HER2-negative patients. Additionally, our study also reveals a significant correlation between ZNF480 expression and clinical parameters, including T, N, M stages, pathologic stage, race, PAM50 subtypes, and receptor status (ER, PR, HER2). The observed correlations suggest ZNF480's crucial role in breast cancer staging, metastasis, and prognosis. Our findings indicate that ZNF480 may influence the progression of breast cancer via the ER, PR and HER2 pathways.

Recent studies highlight that the tumor microenvironment (TME) of breast cancer comprises diverse cellular components, including both innate and adaptive immune responses, with varying clinical significance. Tumor-infiltrating lymphocytes (TILs) are identified as significant biomarkers for breast cancer prognosis and treatment response [20]. Our study found that elevated ZNF480 levels in breast cancer patients are associated with reduced infiltration by several immune cell populations, including aDC, B cells, CD8 T cells, cytotoxic cells, DC, iDC, macrophages, neutrophils, NK CD56bright and CD56dim cells, NK cells, pDC, T cells, Tem, TFH, and Th1 cells. DCs are professional antigen-presenting cells that efficiently capture, process, and present tumor-associated antigens. They activate T cell-mediated immune responses, thereby playing a crucial role in the eradication of tumor cells. A reduction in DC content within the TME may impair the antitumor capacity against breast cancer. This observation aligns with the findings reported by Han E and M. Iwamoto et al. [21, 22]. Similarly, CD8+ T cells possess the capability to directly induce target cell apoptosis, and their positive infiltration has been correlated with prolonged survival in patients with malignancies. This finding has been validated through clinical investigations [23]. Consequently, the diminished infiltration or inhibition of various immune cells, including DCs and CD8+ T cells, within the TME may result in compromised immune responses, thereby facilitating the progression of breast cancer. However, other studies have indicated that the poorer prognosis observed in Luminal BC cases with higher TILs may be attributed to higher tumor grade and distinct cellular composition characterized by Ki67 expression and TIL presence [24]. Thus, the prognosis of breast cancer is influenced not only by the extent of immune cell infiltration but also by the specific composition of these cells. Nonetheless, prior experimental studies have predominantly examined the relationship between immune cell infiltration and breast cancer, while the underlying mechanisms driving changes in the immune microenvironment remain to be elucidated. Our study uniquely investigates the role of ZNF480 in breast cancer progression by modulating immune cell infiltration, which may provide insights into the function of TILs on therapeutic response and patient prognosis.

To elucidate the mechanisms by which ZNF480 influences breast cancer, we conducted a comprehensive analysis of genes associated with high ZNF480 expression, identifying both upregulated and downregulated genes. Gene Set Enrichment Analysis (GSEA) revealed that these genes exhibited consistent expression patterns with ZNF480 and were involved in key biological pathways such as cell nucleus division and metabolism, suggesting a role in tumor progression. Apolipoprotein A2 (ApoA2) plays a pivotal role in lipid metabolism. Recent studies have demonstrated a significant association between ApoA2 and tumor development, indicating its potential as a diagnostic and prognostic marker for certain cancers. For instance, ApoA2 has been identified as a biomarker for pancreatic cancer [25]. ApoA2 may influence the development of breast cancer through its effects on lipid metabolism, anti-inflammatory and antioxidant mechanisms, atherosclerosis, and insulin resistance. Our KEGG analysis suggests that ZNF480 may inhibit ApoA2 expression in the mammary gland, thereby impeding the metabolic transformation of various bioac-

tive compounds and potentially accelerating the progression of breast cancer. Specifically, Hallmark pathway enrichment analysis showed significant upregulation of the protein secretion pathway and downregulation of pathways like angiogenesis and inflammatory response in high ZNF480 samples. C2 pathway analysis indicated significant activation of pathways related to cohesin loading, sister chromatid cohesion, and mitotic cytokinesis in the ZNF480 high expression group, while pathways associated with muscle contraction, envelope formation, and ribosome function were downregulated. These results provide insight into ZNF480's potential molecular mechanisms in breast cancer and highlight potential targets for therapeutic strategies.

Although our study has revealed the expression pattern of ZNF480 in breast cancer and its association with clinical outcomes, there are several limitations and areas that require further investigation. This study primarily utilized bioinformatics analysis to investigate the correlation between ZNF480 expression and breast cancer prognosis. However, large-scale clinical samples are required to validate these findings. Additionally, while numerous Hallmark, Reactome, Wiki, and KEGG pathways associated with ZNF480 expression have been identified, further functional studies are necessary to elucidate the specific roles and interactions of these pathways in breast cancer development.

In conclusion, this study provides a comprehensive investigation into the differential expression of ZNF480 in breast cancer and its correlation with patient prognosis. These findings unveil the precise expression level of ZNF480 in breast cancer tissues and shed light on the underlying molecular pathways involved. These results not only validate the potential role of ZNF480 in breast cancer development but also offer a fresh perspective for comprehending its function within the tumor immune microenvironment.

Acknowledgements

We thank all the families for participating in this research project. This work was supported by Science Foundation of Jiangsu Province Grant (BK20240371); National Science Foundation of China Grant (81901632), and the Jiangsu Province College Students' Innovation and Entrepreneurship Training Program Project (202410285273Y).

Disclosure of conflict of interest

The authors state that they conducted the research without any commercial or financial relationships that could be considered a potential conflict of interest.

Address correspondence to: Jieyu Jin and Bin Feng, Center for Clinical Laboratory, The First Affiliated Hospital of Soochow University, Suzhou 215006, Jiangsu, The People's Republic of China. E-mail: 18912772660@163.com (JYJ); 18962111558@189.cn (BF)

References

[1] Bray F, Laversanne M, Sung H, Ferlay J, Siegel RL, Soerjomataram I and Jemal A. Global cancer statistics 2022: GLOBOCAN estimates of incidence and mortality worldwide for 36 cancers in 185 countries. CA Cancer J Clin 2024; 74: 229-263.

[2] Wilkinson L and Gathani T. Understanding breast cancer as a global health concern. Br J Radiol 2022; 95: 20211033.

[3] Zhang X. Molecular classification of breast cancer: relevance and challenges. Arch Pathol Lab Med 2023; 147: 46-51.

[4] Zhu Q, Liu Z, Cheng X, Liang W, Wang H, Li P, Zhang J, Chen Y, Gao Y and Qian R. ZNF480 influences the prognosis, pathogenesis, and immune microenvironment in patients with lower-grade glioma. Heliyon 2023; 9: e18185.

[5] Sobocińska J, Molenda S, Machnik M and Oleksiewicz U. KRAB-ZFP transcriptional regulators acting as oncogenes and tumor suppressors: an overview. Int J Mol Sci 2021; 22: 2212.

[6] Ye M, Li L, Liu D, Wang Q, Zhang Y and Zhang J. Identification and validation of a novel zinc finger protein-related gene-based prognostic model for breast cancer. PeerJ 2021; 9: e12276.

[7] Shen EH, Overly CC and Jones AR. The Allen Human Brain Atlas: comprehensive gene expression mapping of the human brain. Trends Neurosci 2012; 35: 711-714.

[8] Nguyen DT, Nguyen HH, Nguyen TD, Nguyen TTH, Nakano K, Maejima K, Sasaki-Oku A, Nguyen VB, Nguyen DB, Le BQ, Wong JH, Tsunoda T, Nakagawa H, Fujimoto A and Nong VH. whole genome sequencing of a vietnamese family from a dioxin contamination hotspot reveals novel variants in the son with undiagnosed intellectual disability. Int J Environ Res Public Health 2018; 15: 2629.

[9] Love MI, Huber W and Anders S. Moderated estimation of fold change and dispersion for RNA-seq data with DESeq2. Genome Biol 2014; 15: 550.
[10] Lin K, Wang T, Tang Q, Chen T, Lin M, Jin J, Cao J, Zhang S, Xing Y, Qiao L and Liang Y. IL18R1-related molecules as biomarkers for asthma severity and prognostic markers for idiopathic pulmonary fibrosis. J Proteome Res 2023; 22: 3320-3331.
[11] Zhang S, Lin K, Qiu J, Feng B, Wang J, Li J, Peng X, Ji R, Qiao L and Liang Y. Identification of potential key autophagy-related genes in asthma with bioinformatics approaches. Am J Transl Res 2022; 14: 7350-7361.
[12] Feng B, Zhou T, Guo Z, Jin J, Zhang S, Qiu J, Cao J, Li J, Peng X, Wang J, Xing Y, Ji R, Qiao L and Liang Y. Comprehensive analysis of immune-related genes for classification and immune microenvironment of asthma. Am J Transl Res 2023; 15: 1052-1062.
[13] Zhang Y, Zhou T, Tang Q, Feng B and Liang Y. Identification of glycosyltransferase-related genes signature and integrative analyses in patients with ovarian cancer. Am J Clin Exp Immunol 2024; 13: 12-25.
[14] Subramanian A, Tamayo P, Mootha VK, Mukherjee S, Ebert BL, Gillette MA, Paulovich A, Pomeroy SL, Golub TR, Lander ES and Mesirov JP. Gene set enrichment analysis: a knowledge-based approach for interpreting genome-wide expression profiles. Proc Natl Acad Sci U S A 2005; 102: 15545-15550.
[15] Hänzelmann S, Castelo R and Guinney J. GSVA: gene set variation analysis for microarray and RNA-seq data. BMC Bioinformatics 2013; 14: 7.
[16] Bindea G, Mlecnik B, Tosolini M, Kirilovsky A, Waldner M, Obenauf AC, Angell H, Fredriksen T, Lafontaine L, Berger A, Bruneval P, Fridman WH, Becker C, Pagès F, Speicher MR, Trajanoski Z and Galon J. Spatiotemporal dynamics of intratumoral immune cells reveal the immune landscape in human cancer. Immunity 2013; 39: 782-795.
[17] Yoshihara K, Shahmoradgoli M, Martínez E, Vegesna R, Kim H, Torres-Garcia W, Treviño V, Shen H, Laird PW, Levine DA, Carter SL, Getz G, Stemke-Hale K, Mills GB and Verhaak RG. Inferring tumour purity and stromal and immune cell admixture from expression data. Nat Commun 2013; 4: 2612.
[18] Barzaman K, Karami J, Zarei Z, Hosseinzadeh A, Kazemi MH, Moradi-Kalbolandi S, Safari E and Farahmand L. Breast cancer: biology, biomarkers, and treatments. Int Immunopharmacol 2020; 84: 106535.
[19] Yi Z, Li Y, Ma W, Li D, Zhu C, Luo J, Wang Y, Huang X, Yuan W, Liu M and Wu X. A novel KRAB zinc-finger protein, ZNF480, expresses in human heart and activates transcriptional activities of AP-1 and SRE. Biochem Biophys Res Commun 2004; 320: 409-415.
[20] Dieci MV, Miglietta F and Guarneri V. Immune infiltrates in breast cancer: recent updates and clinical implications. Cells 2021; 10: 223.
[21] Han E, Choi HY, Kwon HJ, Chung YR, Shin HC, Kim EK, Suh KJ, Kim SH, Kim JH and Park SY. Characterization of tumor-infiltrating lymphocytes and their spatial distribution in triple-negative breast cancer. Breast Cancer Res 2024; 26: 180.
[22] Iwamoto M, Shinohara H, Miyamoto A, Okuzawa M, Mabuchi H, Nohara T, Gon G, Toyoda M and Tanigawa N. Prognostic value of tumor-infiltrating dendritic cells expressing CD83 in human breast carcinomas. Int J Cancer 2003; 104: 92-97.
[23] Mahmoud SM, Paish EC, Powe DG, Macmillan RD, Grainge MJ, Lee AH, Ellis IO and Green AR. Tumor-infiltrating CD8+ lymphocytes predict clinical outcome in breast cancer. J Clin Oncol 2011; 29: 1949-1955.
[24] Ciarka A, Piątek M, Pęksa R, Kunc M and Senkus E. Tumor-Infiltrating Lymphocytes (TILs) in breast cancer: prognostic and predictive significance across molecular subtypes. Biomedicines 2024; 12: 763.
[25] Kashiro A, Kobayashi M, Oh T, Miyamoto M, Atsumi J, Nagashima K, Takeuchi K, Nara S, Hijioka S, Morizane C, Kikuchi S, Kato S, Kato K, Ochiai H, Obata D, Shizume Y, Konishi H, Nomura Y, Matsuyama K, Xie C, Wong C, Huang Y, Jung G, Srivastava S, Kutsumi H and Honda K. Clinical development of a blood biomarker using apolipoprotein-A2 isoforms for early detection of pancreatic cancer. J Gastroenterol 2024; 59: 263-278.